Proceeding of the IEEE
International Conference on Robotics and Biomimetics
Dali, China, December 2019

Obstacle Avoidance Control Strategy of a Biomimetic Wire-driven Robot Fish*

Jiayong Chen, Youdong Chen, Binghuan Yu, Ruxu Du and Yong Zhong*

Shien-Ming Wu School of Intelligent Engineering
South China University of Technology
Guangzhou, China

{wijychen, wiydchen, wiyubinghuan}@mail.scut.edu.cn,
{duruxu, zhongyong}@scut.edu.cn

Fengran Xie

Department of Mechanical and Automation Engineering
The Chinese University of Hong Kong
Hong Kong SAR, China

frxie@mae.cuhk.edu.hk

***Abstract* - Fish has attracted the attentions of researchers because of its excellent swimming performance in water, and biomimetic robot fish was then developed. For robot fish, it is quite significant to perceive its surroundings and then take actions automatically due to the unexpected obstacles. In this paper, a wire-driven robot fish, which can detect obstacles, is designed. We adopt Central Pattern Generator (CPG) for motion control of the robot fish which is capable for smooth transitions among different swimming modes. Moreover, an obstacle avoidance control strategy based on a rule base and a closed loop control structure based on PID algorithm are proposed, which can improve the robot fish's perception and reaction abilities to the surrounding environment. Finally, experiments are carried out to examine the feasibility of the proposed control strategy.**

Index Terms – Robot Fish, Central Pattern Generator, Obstacle Avoidance.

I. INTRODUCTION

The ocean covers about 71% of the earth, but it is said that humans have managed to explore only about 5% of the ocean floor due to the uncertain, unpredictable threats in the ocean, and the limitations of human technology. With millions of years of natural selection and evolution, fish gains excellent underwater swimming capacity such as fast swimming speed, high efficiency, low noise and so on, which arouses scientific researchers' interests. In 1994, the world's first robot fish, Robo Tuna, was created at MIT [1]. After that, various robot fishes appeared, which is inspired by different fish species [2-5]. Liu and Hu [6] designed a series of automatic robot fishes named G9, which are based on four IR sensors, the pressure sensor and the accelerometer. Zhou and Low [7] developed a robotic manta ray (RoMan-□), it can perform diversified locomotion patterns by manipulating two wide fins. Inspired by flying insects and swimming fishes, Zhang et al [8] proposed an integrative biomimetic robotic fish, which combined the advantages of insect wings and fish fins to achieve a high maneuverability. There are still other kinds of robot fish protypes, such as 3D swimming robotic fish [9,10], amphibious robotic fish [11], boxfish-like robot [12], soft robotic fish [13], robotic mackerel [14] and so on. Our team has been working on robot fish for many years. In 2011, Li et al [15] first proposed the wire-driven robot fish.

At the beginning of the robot fish study, scientific researchers mainly focus on the structure of the robot fish to mimic real fish swimming and achieve simple cruising and turning motions. But in actual water environment, robot fish must be able to perceive its surroundings and then take actions automatically due to the unexpected obstacles or undercurrents. For instance, robot fish may change swimming orientation and speed according to the obstacles or rise and dive to the desired depth, which can be used to complete specific tasks. Deng et al [16] designed a 3D printed robotic fish using infrared sensors and adaptive neuro-fuzzy control, which can measure the existence of obstacles and simply move away from obstacles. Phuc and Thinh [17] used fuzzy systems on the robot fish to generate robot's path for obstacle avoidance. However, in their robot fish experiments, the robot fish can simply avoid the obstacle without measuring the orientation, speed and other parameters. Korkmaz et al [18] presented a locomotion control of a robot fish based on closed loop sensory feedback CPG model, and carried out the yaw and pitch control experiments to demonstrate the performance. But the control servo motors are coupled, which might make the control difficult.

Based on the wire-driven robot fish, our team has made some progress. Zhong et al [19,20] designed a novel robot fish with a wire-driven active body and a compliant tail. Recently, Xie et al [21] proposed a Central Pattern Generator (CPG) with four input parameters, i.e., the amplitude, the frequency, the offset and the time ratio between two phases forming one turning cycle, the beat phase and the restore phase. This CPG model really makes it convenient to control the robot fish and improves its performance.

The purpose of this paper is to propose an obstacle avoidance control strategy based on the sensor information which enables the robot fish to swim more automatically. The infrared sensors are used to measure the distance between the robot fish and obstacles, which will help indicate whether there are obstacles around the robot. Inertial measurement unit is adopted to gain the yaw angle of the robot fish. In addition, obstacle avoidance rule base and closed loop control structure are presented to improve the performance of the robot fish. Section II presents the mechanical design of the robot fish, electronics and sensors used on the robot fish. The locomotion control CPG mode, obstacle avoidance control design and closed loop control structure are proposed in Section III and

* This work is partially supported by the Fundamental Research Funds for the Central Universities: D2192300.

978-1-7281-6321-5/19//$31.00 ©2019 IEEE

experimental results are shown in Section IV. Finally, conclusions and some future works are given in Section V.

II. Robot System

A. Mechanical Design

As shown in Fig.1, the wire-driven robot fish is composed of head, active body and compliant tail. The active body and compliant tail have been detailed in [19]. In order to protect electronic components against water and get the infrared sensors working, a waterproof transparent shell is used. The sealing rings and bearings are mounted to the shaft, which passing through the shell, to keep out the water while shaft is rotating. On the top of the robot fish, an opening, which is blocked up by a rubber plug, is reserved for the battery charging and program downloading. The propeller of the robot fish is covered and waterproofed by a 3D-printed silicon skin.

The cavity in the head generates huge buoyancy, which makes the robot fish always floating on the water. To balance the gravity and buoyancy, some lead bricks are added inside the head.

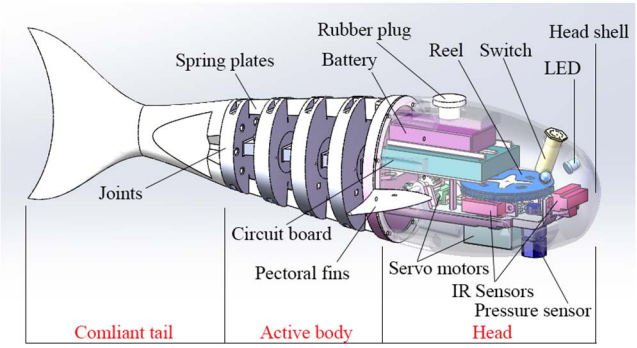

(a)

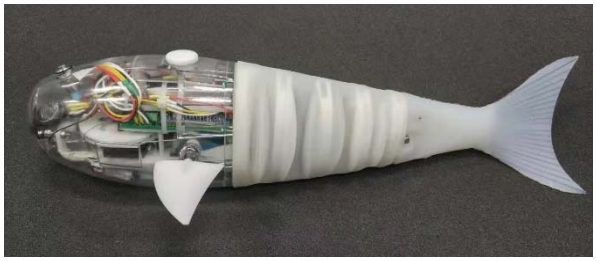

(b)

Fig. 1 (a) Robot fish design, (b) Prototype of the wire-driven robot fish.

B. Electronics and Sensors

Electronics system of the robot fish mainly includes control system, power source, information transmission module, servo motors and sensors. A 7.4V 1500-mAH Ni-H battery is used for power supply of the robot fish with different voltage regulator modules. STM32F103 is used to process information from the sensors and computer, and produce instructions. Radio frequency (RF) wireless module (E62-433T20D) is adopted for the communication between the robot fish and computer or joystick. There are two servo motors, the one named HS-5086WP drives pectoral fins to control robot fish up and down, while the other named SAVOX SW-1210SG drives the active body by the wire ropes.

Inertial measurement unit (IMU, MPU6050) is used to gain the robot fish's acceleration, angular velocity, pitch angle, roll angle and yaw angle. Three are three infrared sensors (GP2Y0A21) in the front, left and right of the base, which can measure the distance between the robot fish and obstacle. The distance range is 10-80cm. The pressure sensor (MS5837) is installed on the bottom outside the shell of the robot fish to obtain the depth of the robot fish. Because of the importance of waterproofing inside the head, a leakage detection module (LD4) is configured on the bottom inside the shell to detect water leakage. If there is a leak, the LEDs turn red.

III. Obstacle Avoidance Control Strategy

A. Locomotion Control: CPG

In nature, fish locomotion is a type of rhythmic motion, which is produced by Central Pattern Generator (CPG). By observing the motion of a black carp, our team proposed a CPG model [21]. The CPG model receives the high-level demands and outputs four parameters, i.e., the amplitude, the frequency, the offset and the time ratio between two phases forming one turning cycle, the beat phase and the restore phase. By changing these four parameters, the robot fish can achieve different motion states. The CPG used in this paper is as followed:

$$\ddot{b} = k_b(0.25k_b(B - b) - \dot{b}) \tag{1}$$

$$\ddot{m} = k_b(0.25k_m(M - m) - \dot{m}) \tag{2}$$

$$\dot{\phi}=[\frac{(1+R)^2}{4R} - \frac{R^2-1}{4R}\text{sign}(\sin\phi)]\omega \tag{3}$$

$$\alpha = b + m\cos(\phi) \tag{4}$$

$$\beta = b + m\sin(\phi) \tag{5}$$

$$\text{sign}(\lambda)=\begin{cases} 1, \lambda > 0 \\ 0, \lambda = 0 \\ -1, \lambda < 0 \end{cases} \tag{6}$$

where b is the offset state, k_b is a positive constant representing the gain of offset, B is the high-level control command of offset, m is the amplitude state, k_m is a positive constant representing the gain of amplitude, M is the high-level control command of amplitude, ϕ is the phase state, R is the time ratio between restore phase (t_r) and beat phase (t_b) of one period as shown in Fig. 2, ω is the high-level control command of frequency, α and β are the outputs of the oscillator.

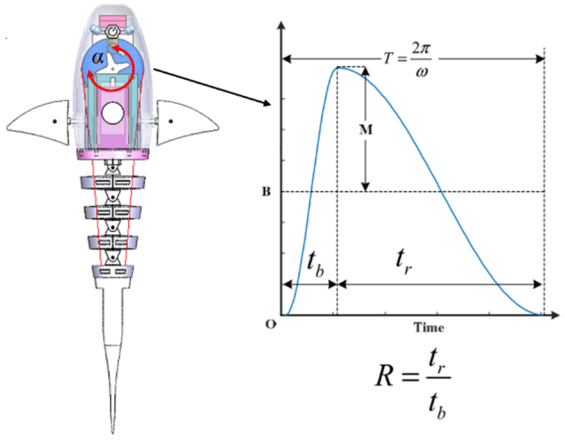

Fig. 2 Illustration of the high-level control command (M, ω, B, R) relating to rotational angle of the servo motor, α.

As shown in Fig. 2, M, ω, B and R are control parameters of amplitude, frequency, offset and time ratio respectively. By

changing these four parameters, the robot fish can cruise and turn with different acceleration, velocity and turning radius. For example, the robot fish cruises forward when $M \neq 0$, $B = 0$ and $R = 1$, on the contrary, it turns when $M \neq 0$, $B \neq 0$ and $R > 1$.

B. Obstacle Avoidance Control Design

The robot fish must be able to avoid the obstacles automatically under unknown circumstance to improve locomotion ability. There are three infrared sensors for detecting the obstacles on the front, left, and right sides of the robot fish respectively. The output information of the IR sensor is continuous voltage corresponding to the distance between the robot fish and obstacle. Therefore, by setting a voltage threshold, the robot fish could identify obstacle at specific distance. The installation positions of these three infrared sensors are shown in Fig. 3 (a). Because of the semitransparent head shell in the infrared path, the IR sensors' output characteristics would be different from them in the air. The left and right IR sensors are bilateral symmetry, thus only one side sensor's output characteristic need to be measured. Taking the left side for example, as shown in Fig. 3 (b), the blue and red lines are front and left IR sensors' output characteristics respectively. The voltage thresholds decrease with the increase of the recognition distance. Due to forward inertia when the robot fish swims, the voltage threshold of the front should be smaller than the left IR sensor, which gives the robot more space to turn when the front IR sensor detects obstacle. Based on the above analysis, we set the voltage thresholds of the front and left IR sensors to 1V and 1.5V respectively, whose corresponding recognition distances are 45cm and 25cm respectively in Fig. 3 (b).

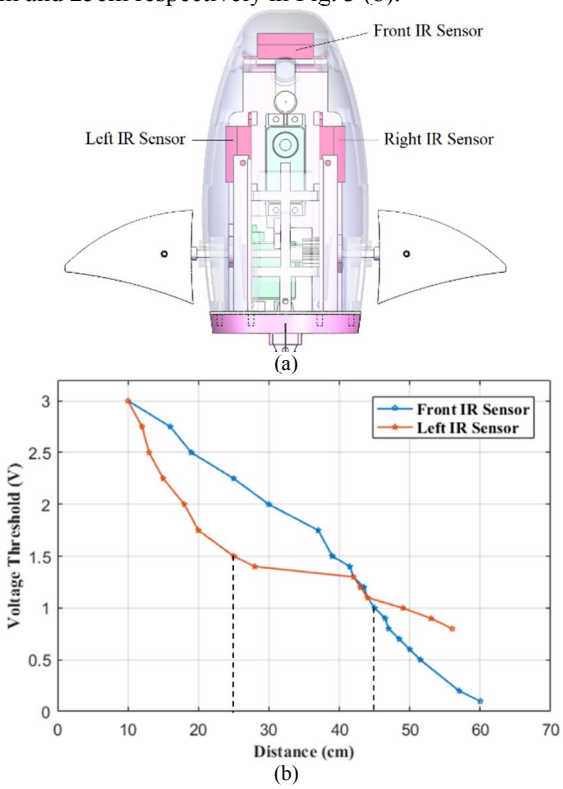

Fig. 3 (a) IR sensors' installation location and working environment, (b) The output characteristics of IR sensors.

The obstacle avoidance control strategy of the robot fish is based on logic control and the data from the sensors. By integrating the information, we build up an obstacle avoidance rule base in TABLE I for the automatically swimming of the robot fish. As shown in TABLE I, F_{IR}, L_{IR} and R_{IR} represent the obstacle information on the front, left and right side of robot fish. The value "0" means there is no obstacle, while "1" means the IR sensor has detected obstacle. The existence of obstacles can be categorized into 8 situations. Based on the idea of logic control, we set up corresponding motion operation for each situation. For example, when there is no obstacle around the robot fish, F_{IR}, L_{IR} and R_{IR} are both set to 0 from the IR sensors information, in which the motion operation of the robot fish is cruising. The rest of the situations are detailed in TABLE I. According to this obstacle avoidance rule base, the robot fish could respond automatically to perceived obstacles.

TABLE I. ROBOT FISH OBSTACLE AVOIDANCE RULE BASE

Condition					Operation
Situation	**F_{IR}**	**L_{IR}**	**R_{IR}**	**Environment description**	**Motion description**
0	0	0	0	No obstacle	Cruise
1	0	0	1	Obstacle on the right	Turn left
2	0	1	0	Obstacle on the left	Turn right
3	0	1	1	Obstacle on the left and right	Cruise
4	1	0	0	Obstacle on the front	Turn left
5	1	0	1	Obstacle on the front and right	Turn left
6	1	1	0	Obstacle on the front and left	Turn right
7	1	1	1	Obstacle both on the front, left and right	Turn right

C. Closed Loop Control Structure

Closed loop control structure has a feedback loop which can reduce or eliminate the deviation. It could be used in our wire-driven robot fish to achieve the robot fish's directional cruising and obstacle avoidance without manual control. The closed loop control structure is divided into two parts, obstacle avoidance and fixed orientation, in Fig. 4.

In the first part, obstacle avoidance, the input signal is three IR sensors' voltage thresholds, and the feedback signal is the data from the output of IR sensors, which contain obstacle situation. The CPG parameters M, ω, B and R are real-time changed by inputting the above two signals into the obstacle avoidance rule base, which enable the robot fish to avoid obstacles.

In the second part, fixed orientation, the input signal is target yaw angle (θ), which refers to the forward angle of the robot fish when it finally cruises steadily. The angle reference coordinate system (0°) is the direction of the robot fish's head when it is energized, and the counterclockwise direction is positive. The feedback signal is yaw angle (ψ), which is the robot fish's real-time swimming direction. But the robot fish's head is constantly swinging when it is swimming due to the approximate sinusoidal oscillation of robot fish in Fig. 2, thus it is difficult to confirm which angle sent back from IMU is the robot fish's swimming direction. In order to address this problem, we set the CPG parameters M, ω and R to 20°, 1Hz and 1 respectively, which can make sure the robot fish's swing is a real sine cure. Then the real-time yaw angle of the robot fish can be obtained by taking the angle collected by IMU at

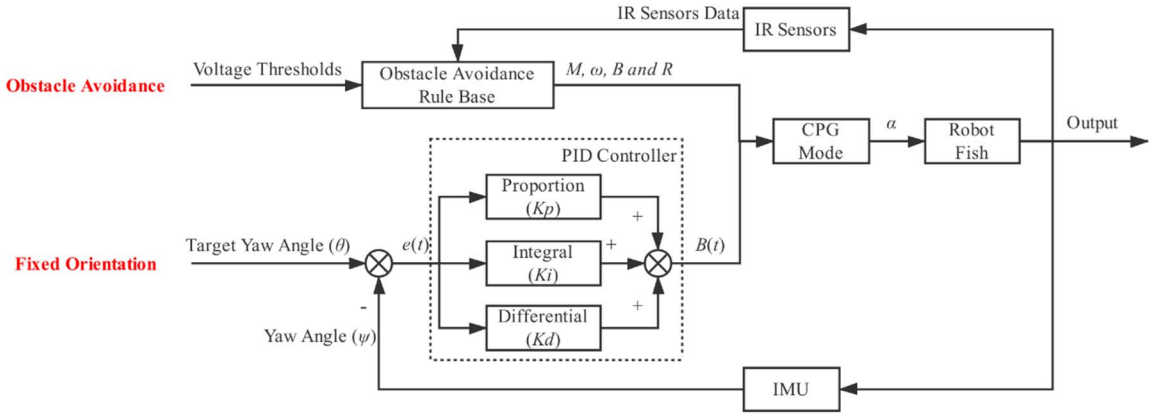

Fig. 4 The closed loop control structure.

the same time interval and taking the mean value in one oscillation period. The deviation signal ($e(t)$) is the difference between target yaw angle and yaw angle, as shown in (7), and is the input of PID controller.

$$e(t) = \theta - \psi \tag{7}$$

The output of PID controller, $B(t)$, is one of the CPG mode input parameters in (8).

$$B(t) = Kp \times e(t) + Ki \times \int_0^t e(\tau)\,\mathrm{d}\tau + Kd \times \frac{\mathrm{d}e(t)}{\mathrm{d}t} \tag{8}$$

In (8), $B(t)$ is the offset of the CPG mode, which is the only changed parameter when robot fish is set to cruise in the fixed orientation. Kp, Ki and Kd are proportional, integral and differential coefficients of PID controller respectively. Before the formal experiment, we carry out a series of simple tests to observe the swimming performance of the robot fish under different PID parameters. Through the analysis of the results, we just adopt proportional and differential control, which could make the robot performing better, and the parameters Kp, Ki and Kd are set to 0.7, 0 and 0.05 respectively. The $B(t)$ value is adjusted in real time according to the PID controller and the deviation between the real-time and the target yaw angle of the robot fish, so that the robot adjusts its own course and swims steadily at the target yaw angle.

IV. Experiments

In this paper, we carry out several experiments to validate the obstacle avoidance control strategy and the closed loop control algorithm based on an experimental platform in Fig. 5. For different experiments, two pools are used, one is 300*200*66cm rectangular, the other is a circular pool with 305cm in diameter and 76cm in height. The camera is installed above the pool to shoot the robot fish swimming in water. The communication between the PC and robot is via RF wireless module, and user interface is programmed using LabVIEW®.

A. Obstacle Avoidance

An experiment is designed to verify the feasibility of aforementioned obstacle avoidance rule base without the closed loop control of yaw angle. The initial parameters of these two experiments are as follow. The CPG mode parameters M, ω, B and R are set to 20°, 1.5Hz, 0 and 1 respectively when the robot cruises straightly; and the parameters are set to 30°, 2Hz, 30° and 1.5 respectively when the robot makes a turn. Based on the analysis in Section III Fig. 3, the voltage thresholds of the front, left and right IR sensors are 1V, 1.5V and 1.5V respectively.

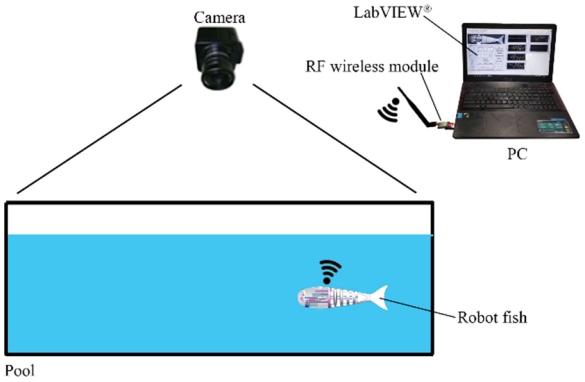

Fig. 5 Experimental platform.

The white rubber plug on the top of the robot fish is used as a marker to depict the swimming track in Fig. 6. At 1.51s, the IR sensor on the left sight of the robot fish detects the blue obstacle, so the robot fish turns slightly to the right. Then it detects wall at 2.21s and avoids hitting the wall successfully at 4s. Next, the robot fish detects the obstacles at 7.18s and 9.15s and reacts automatically according to the obstacle avoidance rule base set before. Through the analysis of the obstacle avoidance experiment, it can be found that the robot fish has been able to detect obstacles independently, and successfully avoid obstacles according to the rule base without any collision.

B. Cruising in a Fixed Orientation

Cruising in a fixed orientation experiments are designed to examine the proposed closed loop control structure on our robot fish. According to the closed loop control structure in Section II, the robot fish continuously adjusts its own course and swims steadily at the target yaw angle on the basis of the deviation between the real-time and the target yaw angle. We set three target yaw angles, 30°, 60° and 90°, to observe whether the robot fish could swim in the given orientation. Before the robot fish starts swimming, other control parameters are set to fixed values. The CPG mode parameters

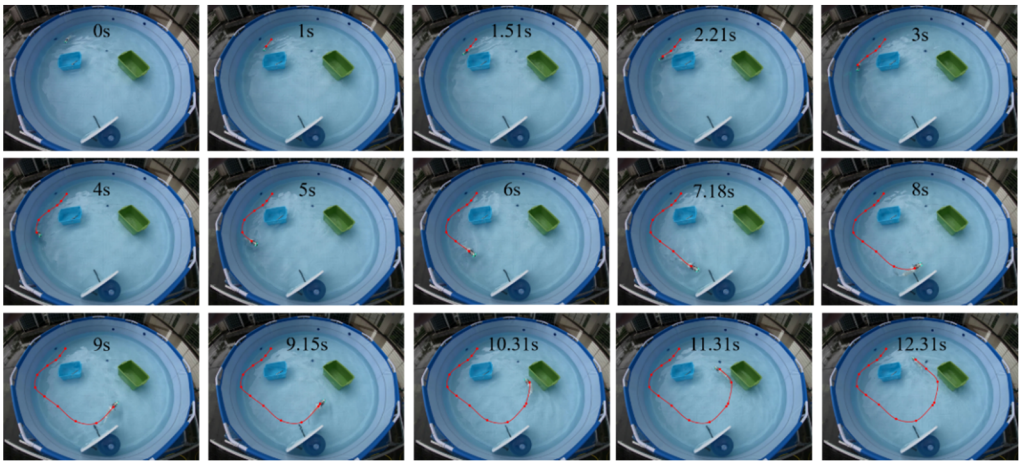

Fig. 6 Sequent pictures of simple obstacle avoidance experiment.

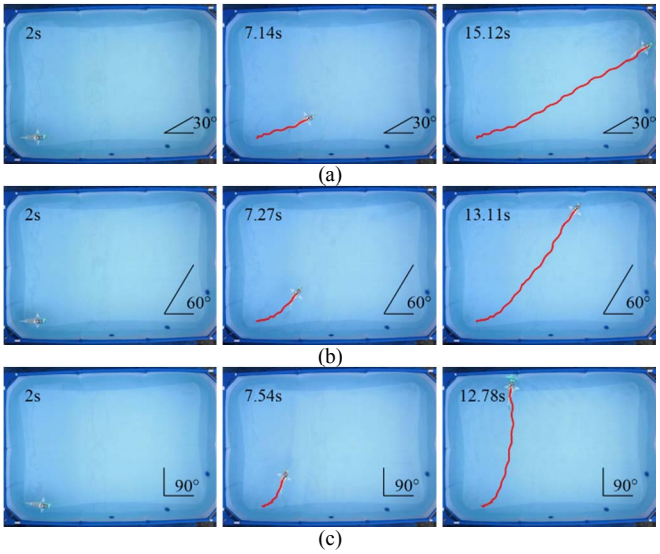

Fig.7 Cruising in the fixed orientation, (a) 30°, (b) 60° and (c) 90°.

M, ω, and R are 20°, 1Hz and 1 respectively, and the PID controller coefficients are 0.7, 0 and 0.05 respectively as shown in Section III. The experiments are carried out three times for each target angle, which might avoid accidental results.

The robot fish's tracks in Fig. 7 obtained by using Kinovea software is very close to the reference orientation when it reaches a stable swimming state.

Furthermore, the real-time yaw angles data sent back from the robot fish are shown in Fig. 8, the blue, red and black lines, whose initial angles both are 0°, are the yaw angles data of 30°, 60° and 90° respectively. The blue one reaches 30° taking just about 1s and has some deviation from 30° in the first few periods, but it can adjust back and stabilize at 30°. As for the red and black lines, it takes about 4s and 5s to reach a relatively stable state with small oscillations at 60° and 90° respectively. Based on the analysis above, it is known that the larger the initial yaw angle is from the target yaw angle, the longer the time to reach the stable swimming state will be.

In Fig. 8, the robot fish's yaw angle swings up and down in sine form at the target yaw angle due to the swinging of the robot fish's head. In each set of experiments, we take three relatively stable periods to obtain the mean values and subtract the target yaw angle to get the error in TABLE II. From the data, we can see that most of errors are relatively small except for a few errors up to ±4°, which is still within the acceptable range. The mean errors are just reach ±2°, which shows the feasibility of our design.

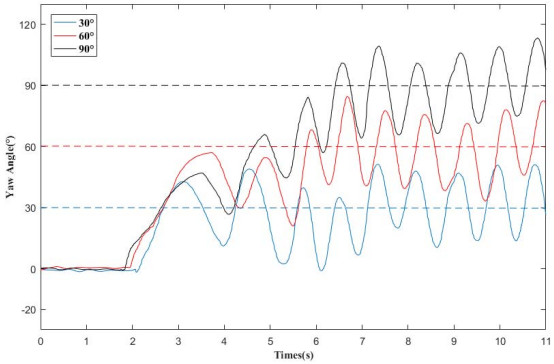

Fig. 8 The real-time yaw angles of the robot fish in a fixed orientation.

TABLE II. ERROR ANALYSIS OF THREE STABLE PERIODS

Angle (°)	Error (°)	Average error (°)	Error variance (°)
30	-0.886	-1.275	7.442
	1.237		
	-4.177		
60	-1.080	1.939	7.285
	2.778		
	4.119		
90	1.239	1.930	0.447
	2.573		
	1.976		

C. *Obstacle Avoidance Under a Fixed Cruising Orientation*

The obstacle avoidance under a fixed cruising orientation experiment is conducted by integrating the above two experiments, obstacle avoidance rule base and closed loop control structure. The target yaw angle is 0°, and we put an obstacle in the robot fish's path to test whether it can avoid the obstacle and then adjust to original orientation. As shown in Fig. 9, the robot fish detects obstacle ahead and begins to turn left at 3.07s. At 5.27s, the robot successfully avoids the obstacle without collision and then starts adjusting its orientation. It takes the robot about 2s to go back to initial orientation.

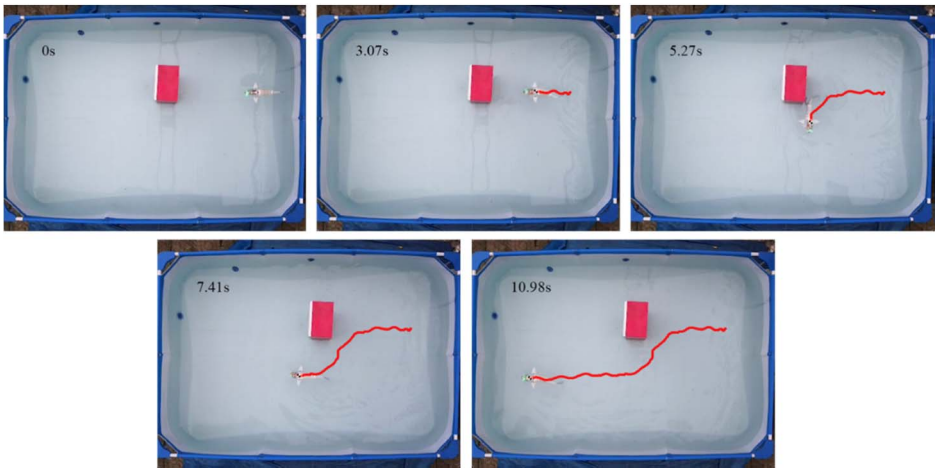

Fig. 9 Obstacle avoidance under a fixed cruising orientation.

V. CONCLUSIONS

In this paper, a wire-driven robot fish is redesigned with an obstacle avoidance control and a closed loop control structure. Experimental results contain an obstacle avoidance experiment, three fixed orientation experiments with different target yaw angle and an obstacle avoidance under a fixed cruising orientation by integrating the above two experiments. All results show that the proposed obstacle avoidance control strategy and closed loop control structure are feasible and efficient. But there are still some limitations, for example, the robot fish may not successfully avoid the complex obstacle due to the influence of head swing on IR sensor detection. The yaw angle error caused by IMU module hardware limitation may increase with the increase of motion time.

In the future work, we will add inertial navigation and GPS system into the robot fish to provide location information on earth and raise accuracy of yaw angle, which will speed up the application of robot fish in the actual water environment.

REFERENCES

[1] M. S. Triantafyllou and G. S. Triantafyllou, "An Efficient Swimming Machine," *Scientific American,* vol. 272, no. 3, pp. 64-70, 1995.

[2] J. Yuan, Z. Wu, J. Yu, C. Zhou and M. Tan, "Design and 3D Motion Modeling of a 300-m Gliding Robotic Dolphin," *Ifac-Papersonline,* vol. 50, no. 1, pp. 12685-12690, 2017.

[3] Z. Wu, J. Yu, J. Yuan and M. Tan, "Towards a Gliding Robotic Dolphin: Design, Modeling, and Experiments," *IEEE/ASME Transactions on Mechatronics,* vol. 24, no. 1, pp. 260-270, 2019.

[4] R. Wang, S. Wang, Y. Wang, M. Cai and M. Tan, "Vision-Based Autonomous Hovering for the Biomimetic Underwater Robot-RobCutt-II," *IEEE Transactions on Industrial Electronics,* vol. 66, no. 11, pp. 8578-8588, 2019.

[5] J. Yu, M. Wang, H. Dong, Y. Zhang and Z. Wu, "Motion Control and Motion Coordination of Bionic Robotic Fish: A Review," *Journal of Bionic Engineering,* vol. 15, no. 4, pp. 579-598, 2018.

[6] J. Liu and H. Hu, "Biologically inspired behaviour design for autonomous robotic fish," *International Journal of Automation and Computing,* vol. 3, no. 4, pp. 336-347, 2006.

[7] C. Zhou and K. H. Low, "Design and Locomotion Control of a Biomimetic Underwater Vehicle With Fin Propulsion," in *IEEE/ASME Transactions on Mechatronics*, vol. 17, no. 1, pp. 25-35, Feb. 2012.

[8] S. Zhang, Y. Qian, P. Liao, F. Qin and J. Yang, "Design and Control of an Agile Robotic Fish With Integrative Biomimetic Mechanisms," in *IEEE/ASME Transactions on Mechatronics*, vol. 21, no. 4, pp. 1846-1857, Aug. 2016.

[9] J. Liu, H. Hu and D. Gu, "A Hybrid Control Architecture for Autonomous Robotic Fish," *2006 IEEE/RSJ International Conference on Intelligent Robots and Systems*, Beijing, 2006, pp. 312-317.

[10] J. Liu and H. Hu, "Biologically inspired behaviour design for autonomous robotic fish," *International Journal of Automation and Computing,* vol. 3, no. 4, pp. 336-347, 2006.

[11] J. Yu, R. Ding, Q. Yang, M. Tan, W. Wang and J. Zhang, "On a Bio-inspired Amphibious Robot Capable of Multimodal Motion," in *IEEE/ASME Transactions on Mechatronics*, vol. 17, no. 5, pp. 847-856, Oct. 2012.

[12] W. Wang and G. Xie, "Online High-Precision Probabilistic Localization of Robotic Fish Using Visual and Inertial Cues," *IEEE Transactions on Industrial Electronics,* vol. 62, no. 2, pp. 1113-1124, 2015.

[13] R. Katzschmann *et al*, "Exploration of underwater life with an acoustically controlled soft robotic fish," *Science Robotics,* vol. 3, no. 16, pp. eaar3449, 2018.

[14] L. Wen, T. Wang, G. Wu and J. Liang, "Quantitative Thrust Efficiency of a Self-Propulsive Robotic Fish: Experimental Method and Hydrodynamic Investigation," *IEEE/ASME Transactions on Mechatronics,* vol. 18, no. 3, pp. 1027-1038, 2013.

[15] Z. Li and R. Du, "Design and analysis of a biomimetic wire-driven flapping propeller," *2012 4th IEEE RAS & EMBS International Conference on Biomedical Robotics and Biomechatronics (BioRob)*, Rome, 2012, pp. 276-281.

[16] X. Deng, D. Jiang, J. Wang, M. Li and Q. Chen, "Study on the 3D printed robotic fish with autonomous obstacle avoidance behavior based on the adaptive neuro-fuzzy control," *IECON 2015 - 41st Annual Conference of the IEEE Industrial Electronics Society*, Yokohama, 2015, pp. 000007-000012.

[17] N. D. Phuc and N. T. Thinh, "A solution of obstacle collision avoidance for robotic fish based on fuzzy systems," *2011 IEEE International Conference on Robotics and Biomimetics*, Karon Beach, Phuket, 2011, pp. 1707-1711.

[18] D. Korkmaz, G. Ozmen Koca, G. Li, C. Bal, M. Ay and Z. H. Akpolat, "Locomotion control of a biomimetic robotic fish based on closed loop sensory feedback CPG model," *Journal of Marine Engineering & Technology,* pp. 1-13, 2019.

[19] Y. Zhong, Z. Li and R. Du, "A Novel Robot Fish With Wire-Driven Active Body and Compliant Tail," in *IEEE/ASME Transactions on Mechatronics*, vol. 22, no. 4, pp. 1633-1643, Aug. 2017.

[20] Y. Zhong, J. Song, H. Yu and R. Du, "Toward a Transform Method From Lighthill Fish Swimming Model to Biomimetic Robot Fish," *IEEE Robotics and Automation Letters,* vol. 3, no. 3, pp. 2632-2639, 2018.

[21] F. Xie and R. Du, "Central Pattern Generator Control for a Biomimetic Robot Fish in Maneuvering," *2018 IEEE International Conference on Robotics and Biomimetics (ROBIO)*, Kuala Lumpur, Malaysia, 2018, pp. 268-273.